



Simulation of Formation Flight Near Lagrange Points for the TPF Mission

Gerard Gómez
Departament de Matemàtica Aplicada i Anàlisi
Universitat de Barcelona
gomez@cerber.mat.ub.es

Martin Lo (Communicating Author)
Jet Propulsion Laboratory
California Institute of Technology
Martin.Lo@jpl.nasa.gov

Josep Masdemont
Departament Matemàtica Aplicada I
Universitat Politècnica de Catalunya
josep@barquins.upc.es

Ken Museth
Computer Science, Graphics Group
California Institute of Technology
kmu@gg.caltech.edu

AAS/AIAA Astrodynamics Specialists Conference

Quebec City, Quebec, Canada July 30-August 2, 2001

AAS Publications Office, P.O. Box 28130, San Diego, CA 92198

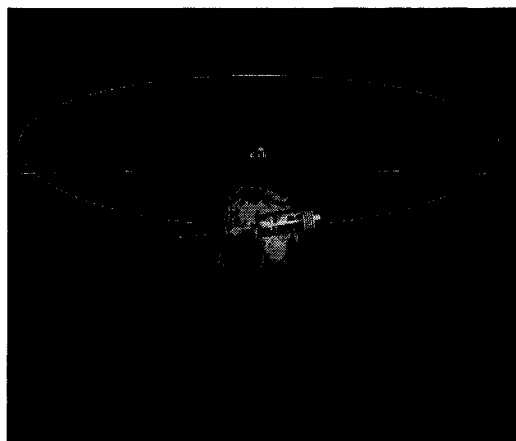
Abstract

The TPF Mission (Terrestrial Planet Finder) is one of the center pieces of the NASA Origins Program. The goal of TPF is to identify terrestrial planets around stars nearby the Solar System. For this purpose, a space-based infrared interferometer with a baseline of approximately 100 m is required. To achieve such a large baseline, a distributed system of five spacecraft flying in formation is an efficient approach. Since the TPF instruments need a cold and stable environment, near Earth orbits are unsuitable. Two potential orbits have been identified: a SIRT-like heliocentric orbit and a libration orbit near the L_2 Lagrange point. In this paper, we focus on the second case: an orbit near the L_2 Lagrange point. Our work in the study of the feasibility of formation flight near the Lagrange points indicates that:

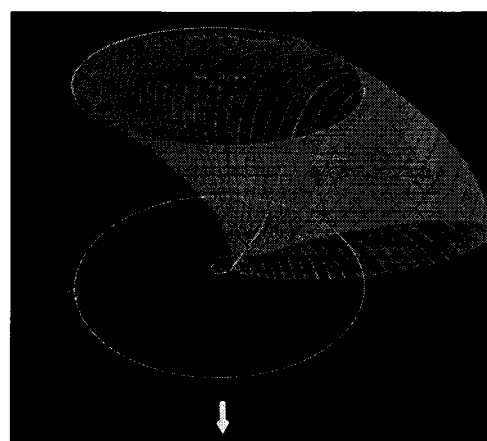
1. Formation flight near L_2 is dynamically possible for the TPF Mission.
2. Linear control around a nonlinear baseline libration orbit near L_2 is adequate for the TPF Mission.

The use of dynamical systems theory not only provides a global view of the phase space showing all the possibilities for the nominal trajectories, but also provides additional structures such as invariant manifolds, that simplify many aspects of the mission analysis such as the transfer from Earth to libration orbit.

1. Introduction



1.1a



1.1b

Figure 1.1a The TPF mothership, carrying the five spacecraft in a low earth orbit. The halo orbit is in the distant about 1.5 million km from the Earth. The Ecliptic is indicated by the blue grid.

Figure 1.1b The TPF transfer trajectory is selected from a family of trajectories on the special surface consisting of free transfer trajectories emanating from the halo orbit about L_2 . The gray orbit around the Earth is the lunar orbit. The yellow arrow points towards the Sun.

1.1 The TPF Mission

The existence of life beyond Earth is a fundamental question for humanity. To answer this question is one the key goals of NASA's Origins Program. The TPF Mission (Terrestrial Planet Finder [1]) is a center piece of the Origins Program to identify Earth-like planets around stars nearby the Solar System where there is potential for life. For this purpose, a space-based infrared interferometer with a baseline of approximately 100 m is required. To achieve such a large baseline, a distributed system of five spacecraft flying in formation is an efficient approach. The current concept has four 3.5 m diameter telescopes, each with its own spacecraft, and a central spacecraft that collects and combines the beams. Since the TPF instruments need a cold and

stable environment, near Earth orbits are unsuitable. Satellites in Earth orbit are exposed to the radiation of the Earth and the Moon. Furthermore, the thermal cycling from the frequent encounter with Earth's shadow creates a thermally unstable environment which is unsuitable for infrared missions. Two potential orbits have been identified: a libration orbit near the L_2 Lagrange point and a SIRTf-like heliocentric orbit. In this paper, we focus on the first case: an orbit near L_2 (see Figure 1.1).

The formation flight problem near the Lagrange points is of great interest. The first constellation in ring formation in an L_1 quasihalo orbit was constructed by Barden and Howell [2] and Barden [3]. Scheeres [4] demonstrated control strategies which looked extremely promising. However, all of these constellations were designed in a loose formation where the shape of the formation is not strictly controlled. In the latter half of FY2000, the Lagrange Committee was formed to study the feasibility of formation flight near L_2 for the TPF mission. Several simulations were performed indicating for the first time that formation flight near L_2 is possible for a TPF-like mission. In this paper, we provide the first simulation of the actual TPF mission orbits about L_2 . The main result is that formation flight near L_2 is dynamically possible for the TPF Mission. More specifically, transfer, deployment, and linear control around a nonlinear baseline libration orbit near L_2 is adequate for the TPF Mission (see Figure 1.2).

1.2 Advantages of a Mission Near L_2

There are several advantages to a libration orbit near L_2 . Such orbits are easy and inexpensive to get to from Earth. Moreover, for missions with heat sensitive instruments (e.g. IR detectors), libration orbits provide a constant geometry for observation with half of the entire celestial sphere available at all times. The spacecraft geometry is nearly constant with the Sun, Earth, Moon always behind the spacecraft thereby providing a stable observation environment, making observation planning much simpler. Since libration orbits will always remain close to the Earth at roughly 1.5 million km with a near-constant communications geometry, the communications system design is simpler and cheaper. The transfer from the Earth to a libration point orbit is cheap and easy, this has two advantages. First, libration orbits require less energy to achieve, hence slightly more mass may be delivered there than to heliocentric orbits. Second, in the event of a failed spacecraft, a replacement spacecraft can be quickly and easily sent to restore the constellation. For a SIRTf-like heliocentric orbit, this could be very costly and may be prohibitive in some instances. Furthermore, libration orbits are excellent staging locations for human presence in space. Consequently, it is feasible for human servicing of missions in libration orbits, but extremely difficult and costly to do so in heliocentric orbits.

1.3 Overview of the Simulations

We model this problem with the Restricted Three Body Problem (RTBP). Solutions within this model are easily moved to the full N-body model with JPL planetary ephemerides. Previous work (see [5]) indicates that the results and conclusion of the simulations are preserved under this model transfer.

In order to study such a complex problem, an interactive simulation environment with constant visual feedback is extremely powerful and convenient. Some of the issues, such as the changing scale of the problem, provide challenges to both the numerical as well as the graphical computations. For instance, the baseline halo orbit has y-amplitudes on the order of 700,000 km. Where as the diameter of the formation is a mere 100 m. Another example is the computation and visualization of the manifolds. Interpolation of points on the manifold for trajectory computations require highly accurate numerics; whereas the interactive visualization requires fast computations of the points on the manifold to support real-time interactions. The successful management of these conflicting requirements is very important to the these simulations.

From the dynamical point of view, the TPF Mission can be broken into four scenarios:

In this paper, we describe the simulations performed for each of the scenarios. We describe the control algorithms and estimate the ΔV required for each of the scenarios. The formation pattern chosen for this study is that of an N-gon as described in the TPF book [1].

2. Orbital Structures Near L₂

For our simulations, all trajectories are integrated with the influence of the planets and the moon using the JPL ephemeris models. However, in order to better understand the possible motions about L₂, it suffices to consider the motions of the RTBP. Experience shows that solutions from the RTPB are readily moved into the full ephemeris model while preserving their salient features. We provide a brief description of the RTBP next. An excellent exposition of the problem is provided by Szebehely [6].

The RTBP describes the motion of a massless particle (spacecraft) in the gravitational field produced by two primaries (e.g. Sun and Earth). In a synodical reference system, the equations of motion can be written as (see [6]),

$$\begin{aligned}x'' - 2y' &= \Omega_x, \\y'' + 2x' &= \Omega_y, \\z'' &= \Omega_z,\end{aligned}$$

where

$$\Omega(x, y, z) = \frac{1}{2} \left((1 - \mu) r_1^2 + \mu r_2^2 \right) + \frac{1 - \mu}{r_1} + \frac{\mu}{r_2}.$$

The RTBP has five libration points, two of them, L₄ and L₅ form an equilateral triangle with the primaries, the other three are collinear with $y=z=0$. If x_{L_j} denotes the value of the x coordinates of L_j, $j=1,2,3$, we will assume that the positions of these points and the primaries are such that

$$x_{L_2} < x_{m_2} = \mu - 1 < x_{L_1} < x_{m_1} = \mu < x_{L_3}.$$

For small values of μ , both $\mu - 1 - x_{L_2}$ and $\mu - 1 - x_{L_1}$ are $3^{-1/3} \mu^{1/3} + O(\mu^{2/3})$ and $x_{L_3} = 1 + O(\mu)$.

We now examine the phase portrait around the collinear equilibrium point L₂ using what is called the reduction to the central manifold (see [7] and [8] for more details). Figure 2.1 below depicts a typical Poincaré section of an energy surface near L₂. This is generated by marking where an orbit near L₂ pierces the XY-plane with $Z' > 0$. The symmetry of the plot is a consequence of one of the natural symmetries of the problem. There are three fixed points corresponding to three periodic orbits. The central fixed point corresponds to the vertical Lyapunov orbit. The two fixed points on the side correspond to the two halo orbits on this energy surface. We note that around the halo orbit, are various rings generated by quasiperiodic orbits around the halo orbit. Quasiperiodic orbits live on tori in the energy surface which when intersected with a plane, produce the rings that we observe around a halo orbit. Similarly, there are quasiperiodic orbits around the vertical Lyapunov orbit.

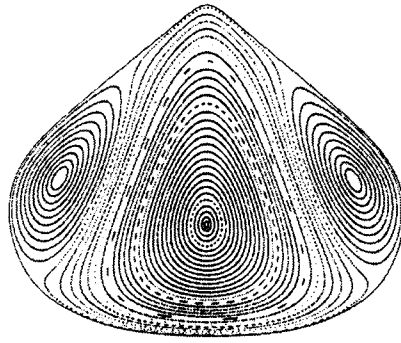


Figure 2.1. Poincare map on the center manifold in the vicinity of L_2 .

This means that around the halo orbit, there are families of quasiperiodic orbits of the same energy from which we can construct trajectories for the formation. However, the problem is that the energy surface also has unstable components. Hence, these quasiperiodic orbits are inherently unstable, just like the halo orbits, and must be maintained. But, also like halo orbits, the maintenance required is inexpensive and infrequent. With this portrait of the phase space region around the halo orbit, we describe next formation flight near L_2 .

3. TPF Mission Simulation Scenarios

3.1 Two Orbital Strategies for TPF

Two basic orbital design strategies for TPF were considered: the Nominal Orbit Strategy, and the Baseline Orbit Strategy. In the Nominal Orbit Strategy, each spacecraft follows its own predefined orbit, called the Nominal Orbit. When the spacecraft deviates significantly from the nominal orbit, control via thruster burns are used to retarget the spacecraft back to the nominal trajectory. In the Baseline Orbit Strategy, a Baseline Orbit, such as a halo orbit, is first computed. The formation trajectories are defined relative to the Baseline Orbit. All controls are targeted the spacecraft back to relative orbits. The Baseline Orbit approach is the sensible strategy to adopt, since the TPF formation changes several times daily. Hence rigid nominal orbits for the formation cannot even be defined rigorously. Note that a Baseline Orbit may have no spacecraft on it.

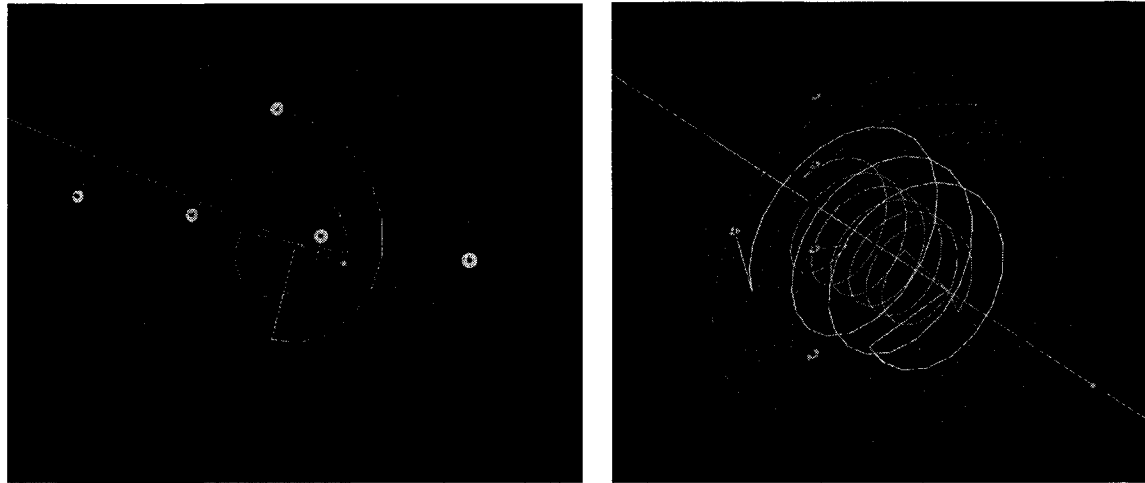
3.2 TPF Mission Phases

TPF Launch and Transfer Phase

For this simulation, we assume the spacecraft starts in a typical 200 km altitude parking orbit at 28.5 deg inclination and a halo orbit is used as a target Baseline Orbit. At the appropriate time, the spacecraft performs a major maneuver of about 3200 m/s. This injects the spacecraft onto the stable manifold of the halo orbit to begin the Transfer Phase. The transfer trajectory is designed by using an orbit of the stable manifold with a suitable close approach to the Earth.

TPF Deployment Phase

It is assumed that all the spacecraft of the formation reach the Baseline Orbit in a single spacecraft. This begins the Deployment Phase. The five satellites are maneuvered to reach their initial positions on the different points of the 20-gon (100m diameter, see Figure 3.1.) at the same time. The Deployment Phase can last several hours. In the simulations to be described in the following sections the deployment time has been taken to be between 1 and 10 hours.



3.1a.

3.1b.

Figure 3.1. The TPF Formation spiraling around the Baseline Halo Orbit (diagonal trajectory). The semi-transparent orange 20-gon is the 100 m diameter of the simulated aperture of the interferometer. The red arrow normal to the 20-gon at its center is the direction of the star currently being observed. The spacecraft and their orbital trails are color coded. The combiner spacecraft and its trail are yellow. In 3.1a., the formation is just starting an observation. In 3.1b, the formation has made an observation for several revolutions and is in the process of reconfiguring for a new observation. The mothership is visible at the lower right hand corner on the halo orbit.

Pattern Maintenance Phase

Once the initial configuration has been established, the spacecraft will maneuver to follow the edge of the 20-gon to provide a suitable spin rate for the formation. The nominal spin rate used for this simulation is 360 deg every 8 hours. The period where the pattern is maintained is called the Pattern Maintenance Phase.

Reconfiguration Phase

Once sufficient data has been acquired for one star system, the formation will be pointed another star for observation. Repointings occur during the Reconfiguration Phase (see Figure 3.1b). The Reconfiguration Phase is similar to the Deployment Phase except the spacecraft do not depart from the same location (i.e. the Mother Ship).

4. Formation Flight Near L_2

The basic concept for the TPF mission is to spin the satellites in an inertial plane with the spin-vector pointed towards a selected star in the sky. For this purpose, we have taken the configuration of five spacecraft specified in the TPF book (see [1]) and represented in Figure 3.1. As explained earlier, to accomplish the mission, a Baseline Orbit approach seems to be the best. We have selected a L_2 halo orbit as a Baseline Orbit. The satellites will be moving in nearby orbits, although none of them will be following the Baseline Orbit at all.

Following the basic TPF concept, a plane which translates in the space according to the base orbit, but always pointing towards a fixed inertial position in the sky, is selected. Inside the plane, each one of the spacecraft follows the edges of a 20-sided N-gon. Essentially, three N-gons are used to build the formation. The outermost one, of diameter D, contains two spacecraft on phases 0 and 180 degrees respectively. The innermost one, of diameter D/3, is in phase with the outermost one and contains two more satellites located respectively on its phases 0 and 180. We

have, in this way, the first four satellites aligned and evenly spaced. The remaining satellite, the collector, is located on phase 0 of a intermediate N-gon of diameter $D/\sqrt{3}$ which in turn has a phase of 270 degrees with respect to the other S/C. This configuration gives us the required geometry for TPF, with D equal to 100m (see Figure 2a).

During the observational periods, the described formation has to be spinning inside the selected plane at the rate of R revolutions per day. A value of R around three, is desired for the TFP mission. Since we are dealing with a non natural motion, pattern maintenance maneuvers have to be performed often to keep this formation. According to the requirements of the mission, these maneuvers have to be done impulsively for each satellite when it reaches each one of the vertex of its corresponding N-gon, in order to target the next vertex in P/N time, were $P=1/R$ is the spinning period of TPF in days.

Using full JPL ephemeris, we have implemented this targeting procedure to obtain the estimates of the impulsive maneuvers, assuming that they are performed without error. The results show that they are practically independent of the base orbit selected. We will keep thinking in a halo base orbit about 100.000 km of Z-amplitude just to fix ideas. The cost of the pattern maintenance in terms of $\Delta V/\text{Day}$ behaves linearly in D and quadratically in R. A suitable rule of thumb that has been found for a satellite being in a 20-gon of diameter D and spinning at the rate of R revolutions per day, is the following:

$$\text{Formation maintenance cost per satellite in cm/s per Day} = 0.0023 * D * R * R.$$

So, for the TFP constellation of diameter D, this is the cost for each one of the outermost, satellites, whist for each one of the innermost ones the cost is 1/3 of this value and, for the collector, the cost is $1/\sqrt{3}$ of the mentioned value. Also, an important point to remark is that the magnitude of each one of the pattern maintenance maneuvers is independent of the vertex (phase) of the N-gon where the satellite is located.

Another important issue in the TPF mission is the estimation of the cost of the deployment of the formation, which in turn will give us preliminary estimations for the cost of reformation, this is the cost of changing the inertial pointing direction of the constellation.

Following again the Baseline Orbit approach, we assume that the satellites have been transferred to the base halo orbit and have to be deployed from a mothership container. Once an initial 20-gon configuration has been selected for the formation, the basic approach consists again in targeting the final destination of each satellite with a desired transfer time, assuming that the departure is done from the base orbit. In the simulations we must assume that all the satellites reach their final destination (the corresponding first vertex of their nominal 20-gon) at the same time. At this time, the first pattern maintenance maneuver should be performed to keep the formation. Otherwise, the satellites should be "stopped" in the vertex waiting for the first pattern maintenance maneuver and the technical complexity, risk and cost of the mission increased. We note that for this purpose the satellites need not depart at once form the mothership, although in the animation of the simulation is presented in this way.

In the simulations we also assume that the deployment is performed using two impulsive maneuvers. The first one is done for the departure of the satellite from the mothership in the base orbit and the second one when the satellite reaches its destination in an N-gon. Because of the fact that just when reaching the first vertex of the N-gon we perform the maneuver to target next one, the second part of the deployment maneuver is not well defined, in the sense that we can only compute the vectorial sum of two maneuvers that are performed together: the N-gon "insertion" plus the first pattern maintenance maneuver. Nevertheless, here we will present estimations of the results associated with the deployment only, correcting for the fact that all the pattern maintenance maneuvers have the same magnitude except for the first one which, when computed, contains also "part" of the deployment procedure.

Let us assume that we want to transfer a satellite from the base orbit to the initial vertex of an N-gon of diameter D which spins at a rate of R revolutions per day. The computations show that the ΔV cost behaves approximately linearly in D, is asymptotic in R and in the deployment time and can be considered independent of the orientation of the N-gon with respect to the base orbit, or equivalently with respect to the inertial pointing direction. In the next table we show suitable rules for some cases:

Table 1. Rules for deployment cost (independent of N-gon orientation)

Deployment Time	R=1	R=3	
1 Hr	$5.5e-2 * D$	$5.6e-2 * D$	cm/s
3 Hr	$1.9e-2 * D$	$2.7e-2 * D$	cm/s
5 Hr	$1.3e-2 * D$	$2.2e-2 * D$	cm/s
10 Hr	$0.9e-2 * D$	$1.8e-2 * D$	cm/s
100 Hr	$0.5e-2 * D$	$1.5e-2 * D$	cm/s

Transfer times between 5 and 10 hours seem appropriate in terms of both, cost and practical implications. Of course 100Hr deployment time is too long for practical applications and it has been included only for illustration of the asymptotic behavior.

As it has been previously said, the process of the reconfiguration of the constellation can be approached in a similar way to the deployment one, except for the fact that the satellites depart from the last vertex of the N-gon instead of from the base orbit. Since the deployment cost is independent of the orientation of the N-gon, when the change of the pointing direction is small, the above table can be used as a rough estimation of the cost changing D for twice the distance between the departure and final vertex, measured in a reference frame moving with the base orbit. Nevertheless better estimates for the reconfiguration cost would have to be done when the selected stars to be examined by TFP had been identified. Of course, a right choice of the sequential order for observation is crucial in the overall mission cost.

In the next table we present an estimation of the ΔV cost associated to satellites located in an N-gon of 50 and 100 m around a L_2 base halo orbit spinning at the rate of 3 revolutions per day and for a 10 year's mission. Halo insertion cost due to transfer from the Earth and station keeping including avoidance of the exclusion zone that could be required in case of using an L_2 Lissajous orbit are also included. The usual station keeping can be assumed absorbed in these often performed pattern maintenance maneuvers. Maneuvers are also considered done without error, so control correction maneuvers are not included.

Table 2. TPF 10 Year Simulation ΔV Budget in 20-Gon spinning at 3 Rev/D

<u>Maneuvers per S/C in m/s</u>	<u>50m Diameter Case</u>	<u>100m Diameter Case</u>
Halo Insertion	5	5
Initial Deployment (10h)	0.009	0.018
Formation Maintenance	0.1/Day	0.2/Day
Station Keeping (Z-Axis)	3/Yr	3/Yr
Reconfiguration (est.)	0.05/Day	0.1/Day
10 Year ΔV Budget (m/s)	585	1135

5. Issues and Approaches of TPF Simulations

The TPF configuration can be classified as a small diameter formation where the transfer is done by means of a mothership inserted into a libration point orbit and followed by the deployment of the satellites. Although the simulations predict no problem in terms of ΔV for the maneuvers to be done during the deployment, a key point that must be addressed in the future is the optimal time

span and sequence of the deployment that avoid the risk of collision, specially when the satellites depart from the mothership.

As we have done in the simulations, the optimal strategy should include the sincronization of the arrival time to each corresponding initial vertex of the N-gon after deployment. Simulations reveal that transfer time doesn't seriously affect the ΔV consumption when chosen in an interval between 3 and 10 hours, so there is a considerable margin of time to design a sequential deployment in such a way that the final synchronization be achieved avoiding the collision problem.

The same approach is valid for the reformation problem, although in this case the risk of collision happens during the excursions of the satellites from its initial position to its final destinations, specially if swapping between the relative positions of the satellites has to be done to keep some homogeneity in the fuel consumption in all the spacecraft. This is something that have to be planned accurately when the possible star targets for TPF have been identified.

In terms of pattern maintenance maneuvers and reformation approach, TPF also requires to put in practice a broader concept of autonomous navigation. Maneuvers have to be done too often to be planned from the Earth. To keep the formation controlled, the suitable approach seems to be that one of the satellites, for instance the combiner, be in charge of measuring the relative positions between the other ones and to order appropriate maneuvers in an automatic way. This strategy decouples the station keeping problem. One leg would be the station keeping of the combiner, that could be even tracked from Earth leaving autonomous navigation concentrated only locally in the formation, and the other one would be the autonomous station keeping of the formation with respect to the combiner. From the experience of our simulations, it seems that due to the big number of maneuvers required, the station keeping could be absorbed by changing slightly the pattern maintenance maneuvers in an automatic way once the combiner has performed an station keeping maneuver planned from Earth, in case that autonomous navigation for the combiner were not implemented. In any case, further simulations including these issues, have to be done in order to estimate the suitable time spans between station keeping maneuvers of the combiner that doesn't imply the change or the addition of new thrusters, and moreover, the station keeping be absorbed by the pattern maintenance maneuvers.

Another important issue for the TPF concept is the size of the maneuvers to be done. Most of them are about 1 mm/s. Are there high precision small thrusters at this level ? We must also take into account that maneuvers will be performed with an error. Even when using high precision thrusters, corrections will have to be applied in order to force the spacecraft to follow their corresponding edge in the N-gon. Again, if we want to have good observational periods, this requires almost instantaneous reaction in the sense of the on board autonomous navigation previously stated. Moreover, correction maneuvers will be in size a fraction of the nominal one, emphasizing again the need of high precision small thrusters.

6. Visualization

The TPF mission design strategies presented in the previous section form a complex problem for which an interactive simulation environment with constant visual feedback is extremely useful. The goals and requirements of the graphics tool for the TPF simulation presented in this paper can be broken into the following steps:

- Animate the time-propagation of the stable manifold of the halo orbit associated with the L2 Lagrange points of the Sun-Earth system
- Select a low-energy transfer trajectory on the stable manifold and compute a conic low-Earth parking orbit for the bus which intersects the manifold trajectory at the selected insertion point

- Launch the spacecraft with TPF satellites from the intersection point of the parking orbit along the low-energy trajectory into the halo orbit
- Once the bus reaches the halo orbit, deploy the 5 satellites into initial formation
- Begin satellite pattern maintenance on a 20-gon by making impulsive burns at the vertex to form a large virtual telescope.
- Satellites make reconfiguration maneuvers to reorient the line of sight by tilting the plane of the 20-gon.

This requirements list for LVIS, the interactive design and visualization tool of the TPF mission, presents a number of graphical problems, which is the topic of the remaining of this section.

6.1 Multi-Scaling Issues

A problem often encountered when visualizing astronomical data is the enormous differences in scale that they typically represent. The differences can be both in spatial distances, time lines for events and relative velocity to some fixed frame of reference. This is especially pronounced in the present case study of the TPF mission. For instance, the baseline halo orbit has amplitudes on the order of 700,000 km whereas the formation flight of the 5 satellites around it has to be accurate to within a few centimeters. Also the velocity of the satellites relative to each other is typically a few meters/hour whereas their relative speed to the halo orbit is several thousand km/hour. The transfer of the bus from a parking orbit around Earth, along a low-energy transfer trajectory, onto the halo orbit takes several months. In contrast, the simulation of the pattern formation of the satellites is typically just for a few hours. These large differences in scales clearly cause problems both for the visualization as well as the numerical simulation. The latter is conveniently solved by partitioning the numerical simulation of the mission into two phases: a computation of the stable manifold in a Sun-Earth rotating frame, and the computation of the satellite motion in a moving frame relative to the baseline halo orbit. This simple but effective strategy suggests a similar stratified approach to the visualization. Thus, the design and visualization of the mission is rendered in two separate windows - one for the transfer from Earth to the halo orbit on a scale of astronomical units (1,500,000 km) and a time-scale of days (step 1 through 3 in the list in section 6) - and one for the formation flight on a scale of meters and minutes (step 4-6). However, one adjustment had to be made to this approach; since the formation flight is simulated in a frame, which moves with a velocity equal to that of the halo baseline this gave a misleading visual illusion of the satellites flying in static periodic orbits around the baseline. To fix this we introduced a new frame of reference in which the camera is fixed, but the satellites move slowly forward and the bus slowly backward. This enabled the visualization of the pattern of the spacecraft formation.

6.2 Parameterization Issues

A fundamental problem when rendering the trajectories is the parameterization. For the numerical simulation a natural parameterization of the trajectories is by time, i.e. $f(t) = (x(t), y(t), z(t))$. Specifically the sampled representations of all the trajectories were given by fixed time-increments. However, due to the rather complex nature of the family of trajectories embedded on the stable manifold in 6D phase-space, such a parameterization is not suitable for visualization - see Figure 6.1.

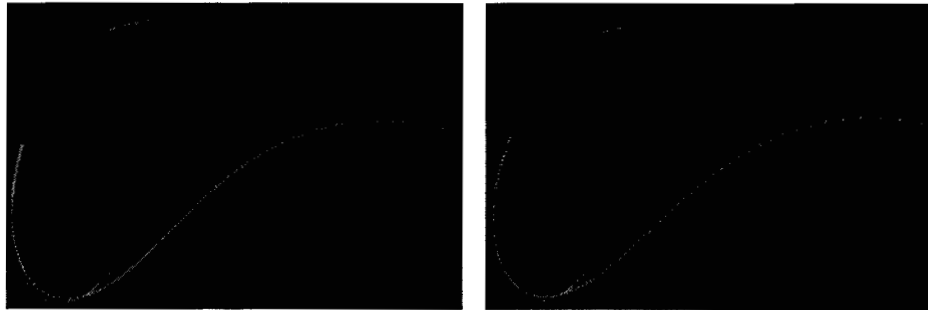


Figure 6.1 Arclength parametrized orbit antialiases the rendering to produce a smooth curve (left), time parametrized does not produce a smooth curve (right).

Since the velocity on the trajectory changes dramatically in space, a time parameterization produces very jagged or aliased lines. On the other hand a fixed arclength parameterization would produce many redundant sampling points in regions near the halo orbit with very low velocity. Thus, we came up with the following scheme for the arclength parameterization of the manifold trajectories which preserves as many of the original points as possible: using the coordinate and velocity information at each pair of two adjacent original sampling points $(x(t_i), y(t_i), z(t_i), v_x(t_i), v_y(t_i), v_z(t_i))$, $i=1,2$, a cubic polynomial is fitted to the corresponding curve

segment. If the arclength $s(t_1, t_2) = \int_{t_1}^{t_2} dt \sqrt{v_x^2(t) + v_y^2(t) + v_z^2(t)}$ is smaller than a given minimum arclength the point at t_2 is removed and if it is integer n times larger than a given maximum arclength new sampling points $i=1, \dots, n$ are inserted at times $t_1 < t_i < t_2$ such that $s(t_1, t_i) / s(t_1, t_2) = i / (n+1)$. The $t_i, i=1, \dots, n$ are numerically found by a Newton-Raphson iteration

of $g_i(t) = s(t_1, t_2) \cdot i / (n+1) - s(t_1, t)$ with $g_i'(t) = \sqrt{v_x^2(t) + v_y^2(t) + v_z^2(t)}$. This simple subdivision algorithm proved efficient for a re-parameterization of the manifold trajectories (see Figure ??), and additionally generates important information about the accumulated arclength along each of the transfer trajectories which is fed back to the user upon selections in step 2 of the list above. However for the triangulation of the manifold tube a different approach had to be employed. As listed as step 1 above the growth of the manifold has to be animated as time evolves which means a time parameterization should be used to ensure a well-defined tube-like geometry of the manifold during all stages of the animation. Furthermore, the subdivision scheme outlined above generates a different number of sampling points for each manifold trajectory. This means a simple triangulation with rings of triangle strip from sets of two connecting points on each trajectory cannot be done easily. On the other hand the original time-parameterized points undersample the tube in regions of space with large velocity (typically near Earth) giving bad aspect ratios of the corresponding triangles. A robust solution was a finer re-sampling of the trajectories in time.

6.3 Semi-Immersive Interaction with Data

The interactive selection of points and trajectories on the manifold (see step 2 in the list above) is a difficult task on a non-immersive desktop monitor. The picking of 3D objects in 2D is typically implemented by intersecting scene objects with a line going through the pin-hole camera and the mouse position on the near viewing-plane. Due to the complicated 3D nature of the trajectories and the fact that thin curves are hard to select accurately by line intersection, we found it extremely useful to employ a semi-immersive device.

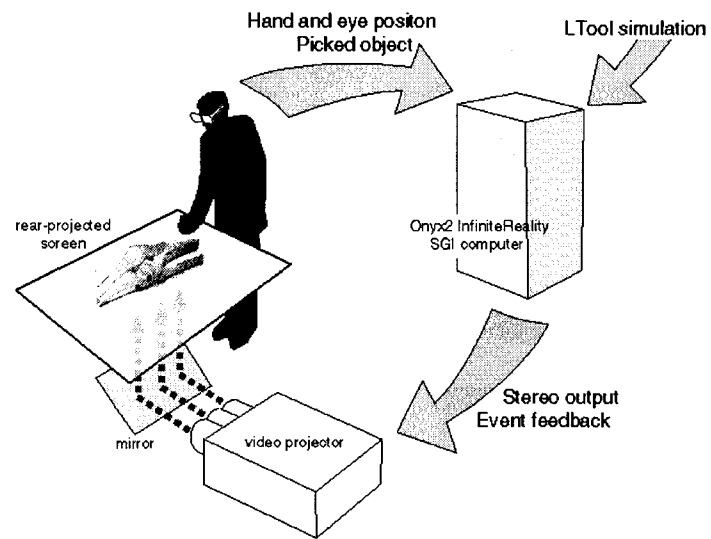


Figure 6.2 Illustration of the Responsive Work Bench at Caltech.

We used a Responsive Workbench which is a 3D interactive virtual reality system with a tabletop metaphor originally developed by Wolfgang Krueger at GMD [9]. The user of the workbench interacts with the virtual objects on the workbench just as they would with actual objects on an actual workbench. Since the Responsive Workbench uses this tabletop metaphor, actual and virtual objects can coexist in the tabletop environment. This creates reinforcing cues and a very natural working environment for many applications. In order to create the 3D environment, users wear shutter glasses (V-sync at 120Hz) to view computer-generated stereoscopic images that are projected the tabletop display surface by a projector/mirror system. The user's head position and orientation are tracked to create the correct perspective for the computer to use when rendering the environment. A 6DOF input device from Polhenus is also tracked by the system allowing the users to interact with objects in the tabletop environment, see Figure 6.3.



Figure 6.3 User interacting with the transfer trajectory on the stable manifold with the Polhenus picking device on the Responsive Work Bench.

6.4 Animation Systems

The physically-based animation is naturally implemented using a procedural approach where the simulation explicitly defines the movements of objects as a function of time. However, to allow for the animation to include objects that were not explicitly included in the actual calculations, (e.g. rotating stars and moon) and to properly synchronize events and phasing of the mission like the growing of the manifold and launch time we also implemented an event-driving scripting system. This allows the user to completely control sequence of events and to "play" the mission forward or backward at any desired speed.

To conveniently communicate a completed mission design by an automated animation or to generate video animations a 3D key frame animations as also implemented. It allows the user to interactively select camera position and orientation at different times of the mission, which are then played back by interpolation between the key frames. Explicitly the camera orientation is represented by quaternions and the interpolation is done as 3 successive spherical cubic interpolations as explained in reference [10,11]. The system then performs off-screen rendering of the scene and dumps the frame-buffer to image files.

6.5 Implementations

An important requirement is that the visualization tool must be interactive on a non-immersive desktop workstation for prototyping, and also flexible enough to be ported to a semi-immersive environment on high-end SGI hardware. The real-time requirement constrains the graphics to only flat or Gouraud-shaded polygons with texture mapping. We select the open-sourced OpenInventor API [12].

6.6 Scene Descriptions And Visual Clues

As emphasized above in section 6.1 it was numerically convenient to stratify the visualization of the TPF mission in two phases or scene graphs - the transfer followed by the formation flight. Common to both scene graphs was a background star-map implemented by projecting the true ephemeris on a rotating sphere placed in the center of the bounding-box. Both scenes also had a directional light source oriented according to the position of the sun in order to obtain the correct lighting of all objects.

The "transfer-scene-graph" had a grid in the XY-plane of the rotating Sun-Earth frame and texture-maps of the spinning Earth with the Moon in a conic orbit around it. The direction of the Sun was indicated by a glowing yellow arrow and the static position of L_2 by a simple colored sphere placed on the Sun-Earth X-axis. The scene also included a texture-mapped bus with 5 satellites attached orbiting around Earth in a conic orbit which by construction intersected the user-selected transfer trajectory. The halo orbit is shown as a closed curve around L_2 , and the stable manifold is shown as a transparent tube and has the embedded family of trajectories twisting around it. After the transfer trajectory is highlighted and the corresponding parking orbit is computed the bus makes a small burn and flies on the stable manifold onto the halo orbit.

The "formation-scene-graph" shows a very small segment of the halo orbit with the bus and 5 satellites attached to it. For this visualization, we had to implement a number of visual and audio cues to emphasize on the rather complex dynamics going on. As already mentioned the illustration of motion relative to the halo orbit had to be artificially introduced, and to enhance this the 5 spiraling trajectories of the satellites were dynamically rendered with color coding. To emphasize on the detailed relative motion of the satellites a transparent 20-gon was added to the scene and the orientation of the virtual telescope was illustrated by an arrow pointing in the line of sight of the IR interferometer. The rocket burns of the satellites at each vertex of the 20-gon were emphasized by short pulsating animations of fire accompanied by a sound effect.

6.7 Lessons Learned and Future Work

We have demonstrated the usefulness of an interactive design, visualization, and animation tool for the TPF mission. Our investigations and prototypes showed the RWB metaphor to be the most useful due to the complex geometry of TPF's trajectories and manifolds. The RWB is able to provide 3D visual cues and nuances absent in non-immersive environments. This is particularly important when the 3D objects are new and unfamiliar since there is no visual reference for comparison from experience. In the case of TPF, this simulation is the first demonstration that a tight formation around a halo orbit is possible. Hence, it is all the more important to provide additional insight through immersive visualization to help the aerospace and scientific communities understand this new design approach.

We solved the multi-scale problems using a stratification approach with multi-windows. We solved the aliasing problems by re-parameterizing the orbits by arclength and by resampling the manifolds in time. We solve the manifold animation problem by propagating the manifold tube in annular strips that are dynamically triangulated. We solved the problem of visualizing the formation pattern by moving the camera in a proper manner. We provided picking on the trajectories and manifolds to enable intuitive and convenient exploration of large data sets. We provided a little scripting language to create efficient 3D key-frame animations using quaternions.

Some of the plans for future work include the computation and visualization of intersections of different manifolds to provide new options for low energy trajectory design. We plan to study the use of haptic devices to add another dimension to the immersive experience. We are also exploring the option of providing semi-immersive capabilities on a desktop workstation for a low-cost alternative to the RWB.

7. Conclusions

Formation Flight Near L_2

The results of the simulations carried out in this paper reveal that formation flight is dynamically possible near L_1/L_2 . Moreover, the base orbit dynamics, station keeping and transfer procedures are well known and have been implemented successfully for single libration point satellites since 1978. For the case of TPF, L_2 is a suitable location, specially for its geometry with respect to Earth and Sun and since the ΔV expenditure is affordable for a mission of a considerable time span. However, formation flight requires new needs as, autonomous on board navigation for station keeping, deployment of the formation, precise pattern maintenance maneuvers, reconfiguration strategies moreover the control of precise formations in the libration point environment. Some of these points have been idealized or excluded from our simulations. So, future important work including all these new issues from an accurate point of view have to be addressed.

Visualization of Formation Flight Near L_2

The visualizations of the different phases of the TPF mission, described in section 5, proved very important for a better understanding of the overall work presented in this paper. The animations were both extremely helpful to explain the essential ideas behind the Lagrange Points dynamics of the mission design, and as a development tool to analyze and exploit the different numerical solutions. However, it was surprisingly challenging to make the physically-based animations visually pleasing.

Especially the scaling issues discussed in detail in section 5.1 initially caused problems, but the implementations of all the animations involved numerous tedious iterations with fine-tuning of shading, light and texture models as well as adding several visual and audio cues to the scene. The port to the Responsive Workbench was relatively straight forward and required few non-trivial changes to the code - the exception being the trick to embed the whole scene in a virtual

bounding box in order for the 6DOF pointing device to have anything of decent size to grab onto. The final animations on the Responsive Workbench gave the extra benefits of a semi-immersive environment and we would like as future work to expand on the degree of interactivity by allowing for the user to directly control the initial conditions of the actual simulation.

Acknowledgments

This work was carried out at the Jet Propulsion Laboratory and California Institute of Technology under a contract with National Aeronautics and Space Administration. The work was supported by the Decade Planning Team, the Terrestrial Planet Finder Mission, and the LTool Project.

References:

- [1] "The Terrestrial Planet Finder, A NASA Origins Program to Search for Habitable Planets", May, 1999, JPL Publication 99-003.
- [2] B.T. Barden and K.C. Howell, Dynamical Issues Associated With Relative Configurations Of Multiple Spacecraft Near The Sun-Earth/Moon L_1 Point, AAS/AIAA Astrodynamics Specialists Conference, Girdwood, Alaska, August 16-19, 1999, Paper No. AAS99-450.
- [3] B.T. Barden, Application of Dynamical Systems Theory in Mission Design and Conceptual Development for Libration Point Missions, Ph.D. Thesis, Purdue University, August, 2000.
- [4] D. Scheeres, Dynamics and Control in an Unstable Orbit, AIAA/AAS Astrodynamics Specialists Conference, Denver, Colorado, August 2000, Paper No. AIAA 2000-4135.
- [5] G. Gómez, K.C. Howell, J. Masdemont and C. Simó. Station Keeping Strategies for Translunar Libration Point Orbits, AAS/AIAA Astrodynamics Conference, Monterey, California, February 1998, Paper AAS98-168, 1998.
- [6] Szebehely, V., Theory of Orbits, Academic Press, 1967, Chapter 1.
- [7] À. Jorba and J.J. Masdemont: Dynamics in the Center Manifold of the Restricted Three Body Problem, Physica D, Vol. 132 1999, 189-213.
- [8] G. Gómez and J.M. Mondelo: The Dynamics Around the Collinear Equilibrium Points of the RTBP, Preprint, 2000.
- [9] Krueger W. and Froehlich B., The Responsive Workbench, IEEE Computer Graphics and applications, May 1994, 12-15.
- [10] K. Shoemake, Animating rotation with quaternion curves, Computer Graphics, volume 19(3), pages 245-54. SIGGRAPH, ACM, 1985.
- [11] K. Shoemake, Quaternion calculus and fast animation, Course Notes, Volume10, pages 101-21. SIGGRAPH, ACM, 1987.
- [12] P. S. Strauss and R. Carey, An object-oriented 3d graphics toolkit, Computer Graphics, volume 26, pages 341-349. SIGGRAPH, ACM, 1992.